Journal of Nuclear Medicine, published on April 18, 2019 as doi:10.2967/jnumed.119.227520

Simplified Methods for Quantification of ^{18}F-DCFPyL Uptake in Patients with Prostate Cancer

Bernard H.E. Jansen[1,2]; Maqsood Yaqub[1]; Jens Voortman[3]; Matthijs C.F. Cysouw[1,3]; Albert D. Windhorst[1]; Robert C. Schuit[1]; Gerbrand M. Kramer[1]; Alfons J.M. van den Eertwegh[3]; Lothar A. Schwarte[4]; N. Harry Hendrikse[1,4]; André N. Vis[3]; Reindert J.A. van Moorselaar[2]; Otto S. Hoekstra[1]; Ronald Boellaard[1]; D.E. Oprea-Lager[1]

[1] Amsterdam University Medical Centers (location VU University Medical Center), Department of Radiology & Nuclear medicine, Cancer Center Amsterdam, the Netherlands
[2] Amsterdam University Medical Centers (location VU University Medical Center), Department of Urology, Cancer Center Amsterdam, the Netherlands
[3] Amsterdam University Medical Centers (location VU University Medical Center), Department of Medical Oncology, Cancer Center Amsterdam, the Netherlands
[3] Amsterdam University Medical Centers (location VU University Medical Center), Department of Anesthesiology, Cancer Center Amsterdam, the Netherlands
[4]Amsterdam University Medical Centers (location VU University Medical Center), Department of Clinical Pharmacology & Pharmacy, Cancer Center Amsterdam, the Netherlands

First author
Bernard H.E. Jansen, MD, PhD candidate
De Boelelaan 1117, 1081 HV Amsterdam
T: 020-4446033
E: bh.jansen@vumc.nl

Corresponding author
Daniela E. Oprea-Lager, MD, PhD
De Boelelaan 1117, 1081 HV Amsterdam
T: 020-4444366
E: d.oprea-lager@vumc.nl

Running title: Quantitative analysis of ^{18}F-DCFPyL PET
Word count: 4363

ABSTRACT

Radiolabeled Prostate-Specific Membrane Antigen (PSMA) Positron Emission Tomography (PET) has demonstrated promising results for prostate cancer (PCa) imaging. Quantification of PSMA radiotracer uptake is desired as it enables reliable interpretation of PET-images, the use of PSMA uptake as an imaging biomarker for tumor characterization, and evaluation of treatment effects. The aim of this study was to perform a full pharmacokinetic analysis of ^{18}F-DCFPyL, a second generation ^{18}F-labeled PSMA ligand. Based on the pharmacokinetic analysis (reference method), simplified methods for quantification of ^{18}F-DCFPyL uptake were validated. **Methods:** Eight patients with metastasized PCa were included. Dynamic PET acquisitions were performed from 0-60 and 90-120 min after injection of a median dose of 313MBq ^{18}F-DCFPyL (range 292-314 MBq). Continuous and manual arterial blood sampling provided calibrated plasma tracer input functions. Time-activity curves were derived for each PCa metastasis and ^{18}F-DCFPyL kinetics were described using standard plasma input tissue-compartment models. Simplified methods for quantification of ^{18}F-DCFPyL uptake (Standardized Uptake Values [SUV]; Tumor-to-Blood Ratios [TBR]) were correlated with kinetic parameter estimates obtained from full pharmacokinetic analysis. **Results:** *N*=46 metastases were evaluated. A reversible two-tissue compartment model was the preferred model for ^{18}F-DCFPyL kinetics in 59% of the metastases. The observed k_4 was small, however, resulting in nearly irreversible kinetics during the course of the PET study. Hence, k_4 was fixated (0.015) and K_i was preferred as the reference kinetic parameter. Whole-blood TBR provided excellent correlation with K_i from full kinetic analysis (R^2=0.97). This TBR could be simplified further by replacing the blood samples with an image-based, single measurement of blood activity in the aorta ascendens (image-based TBR, R^2=0.96). SUV correlated poorly with K_i (R^2 =0.47 and R^2=0.60 for SUV normalized to body weight and lean-body mass, respectively), most likely due to deviant blood activity concentrations (i.e. tumor tracer input) in patients with higher tumor volumes. **Conclusion:** ^{18}F-DCFPyL kinetics in PCa metastases are best described by a reversible two-tissue compartment model. Image-based Tumor-to-Blood ratios were validated as a

simplified method to quantify ^{18}F-DCFPyL uptake and might be applied to clinical, whole-body PET scans. SUV does not provide reliable quantification of ^{18}F-DCFPyL uptake.

Keywords: prostate cancer; ^{18}F-DCFPyL; PSMA; pharmacokinetics; quantification

INTRODUCTION

Prostate cancer (PCa) is the most common cancer in men in the Western world(*1,2*). Positron Emission Tomography (PET) is increasingly used for PCa diagnostics, as it enables early detection of metastases and molecular characterization in vivo. For PCa diagnostics, Prostate-Specific Membrane Antigen (PSMA) binding radiotracers have shown promising results(*3*). PSMA is a class II trans-membrane glycoprotein that provides a valuable target for radiolabeled imaging as its expression is upregulated in malignant prostate cells and is associated with higher tumor grades and risk of disease progression(*4*).

At present, ^{68}Gallium labeled PSMA tracers (half-life 68 minutes) have been studied most extensively(*3,5*). Alternatively, ^{18}Fluorine labeled tracers have been developed, for example 2-(3-(1-carboxy-5-[(6-^{18}F-fluoro-pyridine-3-carbonyl)-amino]-pentyl)-ureido)-pentanedioic acid (^{18}F-DCFPyL), a second generation small-molecule ligand with strong PSMA binding characteristics(*6,7*). The ^{18}F-radionuclide provides a higher PET-image resolution compared to ^{68}Ga, due to a shorter positron range and higher positron yield(*3*). This may improve detection of PCa metastases, as was demonstrated in a head-to-head comparison between ^{18}F-DCFPyL and ^{68}Ga-PSMA PET/CT(*8*). Additionally, the longer half-life of ^{18}F (110 minutes) allows centralized, large-scale production of the PSMA tracer.

In clinical practice, PET scan evaluation is mostly performed by visual assessment or by using semi-quantitative measurements of tracer accumulation (Standardized Uptake Values [SUV]). However, visual assessment is intrinsically observer-dependent and semi-quantitative measures should be carefully validated first, as they do not always reflect the tracer's pharmacokinetics(*9*). To ensure reliable evaluation of ^{18}F-DCFPyL PET images, accurate quantification of ^{18}F-DCFPyL uptake is thus desired. Moreover, quantification of ^{18}F-DCFPyL uptake may serve as an imaging biomarker for tumor characterization (e.g. histologic grade or prognostic outcome), and allow evaluation of treatment response.

The most elaborate and accurate method for quantification of tracer uptake is pharmacokinetic modelling based on dynamic PET acquisitions and plasma input functions, requiring (metabolite-corrected) arterial blood sampling(*10*). The complexity of these procedures and the related patient discomfort make full pharmacokinetic modelling unsuited for daily clinical practice. Hence, simplified methods are needed to approximate full quantitative analysis. In this study we aimed to validate simplified methods for quantification of ^{18}F-DCFPyL uptake against results from pharmacokinetic analysis, in patients with PCa.

MATERIALS AND METHODS

Patients

Eight patients were included in the Amsterdam UMC between February and August 2018. Inclusion criteria were: (1) histologically proven PCa; (2) two or more thoracic metastases (detected by routine clinical imaging studies, performed maximally 3 months prior to the study); and (3) at least one metastasis of ≥1.5cm in size (to minimize partial volume effects). Thoracic metastases were required to allow PET imaging of both tumor tissue and the aorta ascendance (blood activity) within a single Field-of-View. Patients with multiple malignancies and claustrophobia were excluded.

The study has been approved by the ethical review board of the Amsterdam UMC and all subjects signed an informed consent. This trial was registered under EudraCT number 2017-000344-18 and NTR 6477.

Synthesis of ^{18}F-DCFPyL

^{18}F-DCFPyL was synthesized under Good Manufacturing Practices conditions at the Amsterdam UMC (Radionuclide Center), using the precursor of ABX (ABX GmbH®, Germany). Details are provided in Supplemental Text 1(*11,12*).

Imaging Protocol

Patients were not required to fast prior to the scan. Image acquisitions were performed using an EARL calibrated Philips Ingenuity TF PET/CT scanner (Philips Healthcare®, the Netherlands/USA). The scanner's axial field-of-view (FOV) was positioned over the thoracic metastases as well as the ascending aorta (to evaluate image-based blood activity concentrations). The protocol started with a low-dose CT (50 mAs, 120 kV) followed by a dynamic PET scan from 0-60 min post-injection (p.i.) of ^{18}F-DCFPyL (median dose 313 MBq, range 292-314). We intended to perform full pharmacokinetic analysis up until 120 min

p.i., since previous studies demonstrated improved visual interpretation and higher tumor SUV at later time points(*13,14*). Performing dynamic acquisitions continously for 120 min did not seem feasible due to patient discomfort, however. Hence, a 30 min break was implemented after the first 60 min dynamic scan. The protocol continued with another low-dose CT and 30 min dynamic scan at 90-120 min p.i.

Dynamic PET data were binned into 19 frames for the first dynamic ^{18}F-DCFPyL scan (6x5, 3x10, 4x60, 2x150 and 4x300 seconds) and 6 frames for the second dynamic scan (6x300 seconds). Data were corrected for decay, dead-time, scatter, and random coincidences; photon-attenuation correction was performed using the low-dose CT scans. PET data were reconstructed using the default BLOB-OS-TF reconstruction algorithm providing images with a matrix of 144 by 144 by 45 voxels and with an isotropic voxel size of 4 mm.

Continuous arterial blood sampling was performed during the first ^{18}F-DCFPyL PET scan (0-60 min p.i.) using an automated blood sampler (Veenstra Instruments)(*15*). Manual arterial blood samples were taken at 5, 10, 20, 30, 40, 60, 100, 110, and 120 min; manual venous samples were taken at 10, 30 and 60 min. Whole-blood and plasma activity concentrations were measured, as well as parent and metabolite fractions of ^{18}F-DCFPyL. Metabolite analysis was performed using high-performance liquid chromatography.

Data Analysis

The PCa metastases were delineated on the summed image-frames from the last 15 min of the first ^{18}F-DCFPyL scan (45-60min p.i.). A 50% isocontour of SUV_{peak} (sphere of 1.2 cm diameter, positioned to maximize its mean value) with correction for local background uptake was used to obtain volumes of interest (VOIs)(*16*). The obtained VOIs were imported to the second ^{18}F-DCFPyL scan and manually repositioned over the metastases. Time courses of radioactivity concentrations (time-activity curves [TACs]) were produced for each VOI for the entire length of the dynamic ^{18}F-DCFPyL scan. In addition,

image-based blood activity concentrations (blood pool TAC) were assessed using a 3 by 3 voxel VOI placed in the ascending aorta in 5 consecutive slides(*17*).

Pharmacokinetic Modelling

Pharmacokinetic properties of radiotracers are explained using kinetic models, typically including one or two tissue compartments (T) that are linked to the arterial blood compartment (tracer input) by kinetic rate constants (*k*). Examples include the irreversible two-tissue compartment model, which is applicable to tracers being trapped into the target tissues (e.g. ^{18}F-FDG), and the reversible two-tissue compartment model, often applicable to receptor binding radiotracers(*18,19*).

Continuous arterial sampling data were used to provide tracer input functions. The continuous sampling curves were both calibrated (2.5-60 min) as well as extrapolated using multi-exponential fit (60-120 min) based on whole blood activity concentrations from the manual arterial samples. The curves were corrected for plasma-to-whole blood ratios. The final blood input functions were corrected for delay to compensate for differences in tracer arrival time in the tumor and at the online detector.

Pharmacokinetic modelling was performed with in-house developed software in MATLAB (MathWorks Inc.), using non-linear regression analysis(*19*). ^{18}F-DCFPyL data were described using standard several pharmacokinetic models (reversible single tissue-compartment model; reversible and irreversible two-tissue compartment model), all with blood volume fraction parameter (V_b, consisting of whole-blood activity)(*10*). Net influx rate (K_i) and volume of distribution (V_T) were calculated from the derived kinetic rate constants, as follows:

$$\mathrm{K_i} = \frac{\mathrm{K_1} * k_3}{k_2 + k_3}$$

$$\mathrm{V_T} = \frac{\mathrm{K_1}}{k_2} * (1 + \frac{k_3}{k_4})$$

Lastly, several simplified uptake measures were produced: (A) Patlak K_i (t* = 30 min p.i.); (B) Logan V_T (t* = 30 min p.i.); (C) SUV normalized to both bodyweight (SUV_{BW}) and lean body mass (SUV_{LBM}); (D) SUV normalized to the area under the whole blood input curve (SUV_{AUC}); (E) tumor-to-blood ratio (TBR). Several SUV intervals were analyzed (30-60 min, 100-120 min, 110-120 min). TBR was derived by normalizing the mean tumor uptake (Bq/cc) with the (time-matched) arterial blood activity concentration (Bq/cc). To further simply the TBR, we assessed whether the blood samples could be replaced by an image-based, whole-blood activity measurement from the ascending aorta (*i.e*. an *image-based TBR*). Image-based TBR were derived by normalizing mean tumor uptake (either Bq/cc or SUV) with the mean activity in the arterial blood pool (Bq/cc or SUV), see Figure 2. In clinical whole-body PET acquisitions, the ascending aorta is within FOV around half-way the duration of the scan. To reflect this scenario, we used the uptake in the aorta as measured during the middle frame of the last dynamic scan (105-110 min p.i.) for our analysis of an image-based TBR.

Statistical Analysis

Normality of the data was assessed visually using histogram analysis. The Akaike criterion was applied to select the preferred pharmacokinetic model for ^{18}F-DCFPyL (*20*). Each simplified measure was compared to the parameters derived from full kinetic modelling by linear regression analysis (R^2). Significance level was set a $p<0.05$. Statistical analyses were performed with SPSS 22.0 (IBM®, USA).

RESULTS

Eight patients were enrolled, with a median PSA of 473 ng/ml (range 1.7-2792) at the time of scan (Table 1). Seven patients had metastatic castration-resistant prostate cancer (mCRPC) and received androgen deprivation therapy at the time of scan. All of these patients had received prior treatment with docetaxel and five patients had also received enzalutamide or abiraterone. One patient was recently diagnosed with metastatic (recurrent) PCa after radical prostatectomy and had not received any systemic treatment yet.

Pharmacokinetic Analysis

Plasma-to-whole blood activity ratios were stable over time in all patients and no metabolites of ^{18}F-DCFPyL were detected in the blood samples (see Supplemental Figs 1-3), hence no metabolite correction of the tracer input functions was needed. *N*=46 metastases were evaluated (41 bone metastasis, 5 lymph node metastases). Based on the Akaike criterion the reversible two-tissue compartment model was the preferred model to describe tracer kinetics in 27 metastases (59% of total), followed by the reversible single-tissue model in 16 metastases (35%) and the irreversible two-tissue model in 3 metastases (7%). A typical example of ^{18}F-DCFPyL uptake in a PCa metastasis and normal tissues is given in Figure 1. Although the reversible two-tissue compartment model provided the best description of the tracer's kinetics, the detected k_4 values were small (<0.05), resulting in instable fits (i.e. relative SD of V_T >100%). Multiple rounds of kinetic modelling were performed, with increasingly stringent kinetic boundaries. Ultimately, k_4 was fixed at 0.015, which led to stable kinetic parameters in all but one metastasis (which was censored). Given the small and fixed k_4 value, K_i derived from the reversible two-tissue compartment model was preferred as the macro-kinetic parameter for further evaluation of ^{18}F-DCFPyL uptake quantification (instead of V_T). The derived kinetic parameter estimates and simplified methods are shown in Table 2.

Validation of Simplified Methods

TBR based on arterial whole-blood sampling provided the best correlation of the simplified methods with K_i from the reversible two-tissue compartment model (Table 3). The even more simplified *image-based TBR* had a similarly high correlation to K_i as the TBR based on arterial blood samples (R^2 = 0.96 versus R^2 = 0.97 respectively, Table 3)(Fig. 3).

In our cohort, SUV and K_i correlated poorly (both SUV_{bw} and SUV_{lbm}, Table 3). On an individual patient level, apparent relations between SUV and K_i were observed, yet the slope of these individual relations was clearly different between subjects (resulting in a poor correlation of SUV with K_i overall) (Fig.4).

DISCUSSION

In this study we performed a pharmacokinetic analysis of ^{18}F-DCFPyL uptake in PCa metastases, based on dynamic scan acquisitions and arterial blood activity input. A reversible two-tissue compartment model (with a fixed, small k_4) was found to best describe the kinetic behavior of ^{18}F-DCFPyL. In this model K_1 and k_2 may explain the transport and (un)binding of ^{18}F-DCFPyL from the blood stream to the prostate cancer cells. Upon binding to the extracellular part of the target, PSMA-ligands are known to be internalized into the cell(*6*), a (reversible) process which may described by the observed k_3 and k_4.

Full pharmacokinetic analysis is considered the reference method for tracer uptake quantification, but is not feasible in daily clinical practice. Hence, validation of simplified methods for accurate quantification of ^{18}F-DCFPyL is needed for use in standard whole-body PET acquisitions. Of the simplified metrics, we found the image-based TBR to provide an optimal trade-off between accurate representation of the underlying tracer kinetics versus simplicity of the required scan procedure.

An image-based TBR can be easily obtained from static whole-body acquisitions without the need for additional blood sampling. A single blood activity measurement in the ascending aorta suffices to normalize the uptake of detected PCa metastases (Fig.2). The image-based TBR provides a practical way to quantify tumor tracer uptake and compare the uptake of metastases in different patients, which may ultimately allow standardization of PET scan interpretation. Moreover, this simplified quantitative analysis may serve as an imaging biomarker, as PSMA-expression is found to correlate with histologic grade and disease progression. Lastly, the TBR may provide a means to monitor treatment response, as changes in TBR could imply therapeutic response or failure. Further research is needed to establish the validity of TBRs for these possible applications.

^{18}F-DCFPyL uptake in PCa metastases rises continuously during the first 2 hours after injection, while background activity decreases (Fig. 1). Hence, the contrast between tumor and background will

increase over time, facilitating detection of additional metastases. These findings support the observations by Wondergem et al.(*13*), who demonstrated that the detectability of metastases was higher at an uptake interval of 120 min p.i. compared to 60 min p.i. In fact, tumor contrast is likely to rise even after 120 min p.i.; the visual benefit of starting PET acquisitions at even later time points might be offset by decreasing image-quality due to a loss of radioactivity (decay), however.

Compared to TBR, SUV would provide an even more simplified method for quantification of ^{18}F-DCFPyL uptake, as no assessment of the blood activity is needed. However, our results clearly indicate that no reproducible relation between SUV and K_i exists (see Table 3 and Fig. 3). The varying relation between SUV and K_i that we observed between patients may be explained by differences in the blood pool activity concentration (i.e. the tracer input function). Patient 5 demonstrated the most divergent relation of SUV and K_i (Fig 3.) and this patient's blood activity concentration was noticeably below average (both from arterial sampling, as well as image-based measurements, see Supplemental Fig. 3). The low blood activity in this patient may in turn be explained by a vast total tumor burden, as metastases were identified in nearly all imaged bone structures. Patient 7 appeared to be a similar case (extensive tumor volume; lower blood activity concentration; divergent relation of SUV to K_i). Overall, these findings imply that SUV is an inaccurate method to quantify ^{18}F-DCFPyL uptake and explain why a method that normalizes for blood activity concentration (i.e. TBR) provides the best correlation to full kinetic analysis.

TBRs were found to continuously rise over time (Fig. 2), which entails that TBRs are affected by differences in the duration of the applied scanning protocol between and within centers. To reliably compare TBRs between institutes and at different time points (e.g. before and after therapy), it is pivotal that the time between tracer injection and image-acquisition is strictly standardized. Hence, we strongly recommend to harmonize the uptake interval (e.g. 120 min p.i.), direction of scanning (e.g. "feet-first"),

and the overall whole-body scan duration between centers and ensure strict adherence to the imaging protocol.

Our study has some limitations. Firstly, the complexity of full kinetic analysis and the associated patient discomfort did not allow inclusion of many patients, which precluded subgroup analysis (e.g. primary metastatic patients versus mCRPC patients). Secondly, a heterogeneous population of patients with metastasized PCa was included (e.g. PSA ranged from 1.7-2792 ng/ml), with therefore potentially varying levels of PSMA expression on the examined metastases. Furthermore, almost all patients were treated with ADT, which is known to influence PSMA expression(*21*). Although absolute tumor tracer uptake may be subject to differences in PSMA expression, it is unclear if this has a strong effect on the kinetic behavior of ^{18}F-DCFPyL. In our study, tumor TACs and kinetic outcomes showed a fairly consistent pattern across all subjects, despite their heterogeneous disease. Lastly, TBR is the preferred simplified method, yet its daily variation within patients remains unknown. Further research is desired to establish the repeatability of TBR and allow reliable assessment of treatment response.

CONCLUSION

The pharmacokinetics of ^{18}F-DCFPyL in patients with metastasized PCa are best described with an irreversible two-tissue compartment model with a fixed k_4. Tumor-to-blood ratios based on a single blood activity measurement in the aorta ascendens (image-based TBR) provide an accurate simplified method to assess ^{18}F-DCFPyL uptake in PCa metastases. Image-based TBRs can be used to quantify ^{18}F-DCFPyL uptake in clinical, whole-body PET/CT scans and may be used as an imaging biomarker for tumor characterization or to evaluate treatment response. Standardized Uptake Values (SUV) should not be used to quantify ^{18}F-DCFPyL uptake as this metric is not able to account for variations in the blood input function across patients.

Tumor tracer activity concentration increased over time, while background activity decreased. Although these findings are based only on 8 patients, they are consistent with previous research suggesting diagnostic benefit of performing ^{18}F-DCFPyL PET examination at later time points after tracer administration (e.g. 120 min).

DISCLOSURES

Dr. R. Boellaard reports to have a scientific collaboration with Philips Healthcare. The other authors have no disclosures or potential conflicts of interest to this manuscript.

ACKNOWLEDGMENTS

We gratefully acknowledge the Cancer Center Amsterdam for the research grant that funded this study (CCA2016-5-30).

KEY POINTS

QUESTION: What are accurate simplified methods to perform quantitative evaluation of ^{18}F-DCFPyL PET/CT in clinical practice?

PERTINENT FINDINGS: Full pharmacokinetic analysis of ^{18}F-DCFPyL (reference method) was performed in eight patients with metastatic prostate cancer, revealing a reversible two tissue-compartment model as the preferred kinetic model. This full quantitative analysis could be simplified by using image-based Tumor-to-Blood ratios, but not with Standardized Uptake Values.

IMPLICATIONS FOR PATIENT CARE: Tumor-to-Blood ratios (and not Standardized Uptake Values) can be used as a simplified method to perform quantitative evaluation of ^{18}F-DCFPyL PET/CT, enabling reliable interpretation of PET-images and the use of tracer uptake as an imaging biomarker.

REFERENCES

1. Siegel RL, Miller KD, Jemal A. Cancer statistics, 2019. *CA Cancer J Clin.* 2019;69:7-34.

2. Ferlay J, Colombet M, Soerjomataram I, et al. Cancer incidence and mortality patterns in Europe: Estimates for 40 countries and 25 major cancers in 2018. *Eur J Cancer.* 2018;103:356-387.

3. Rowe SP, Gorin MA, Allaf ME, et al. PET imaging of prostate-specific membrane antigen in prostate cancer: current state of the art and future challenges. *Prostate Cancer Prostatic Dis.* 2016;19:223-230.

4. Perner S, Hofer MD, Kim R, et al. Prostate-specific membrane antigen expression as a predictor of prostate cancer progression. *Hum Pathol.* 2007;38:696-701.

5. Perera M, Papa N, Christidis D, et al. Sensitivity, Specificity, and Predictors of Positive 68Ga-Prostate-specific Membrane Antigen Positron Emission Tomography in Advanced Prostate Cancer: A Systematic Review and Meta-analysis. *Eur Urol.* 2016;70:926-937.

6. Robu S, Schmidt A, Eiber M, et al. Synthesis and preclinical evaluation of novel (18)F-labeled Glu-urea-Glu-based PSMA inhibitors for prostate cancer imaging: a comparison with (18)F-DCFPyl and (18)F-PSMA-1007. *EJNMMI Res.* 2018;8:30.

7. Chen Y, Pullambhatla M, Foss CA, et al. 2-(3-{1-Carboxy-5-[(6-[18F]fluoro-pyridine-3-carbonyl)-amino]-pentyl}-ureido)-pen tanedioic acid, [18F]DCFPyL, a PSMA-based PET imaging agent for prostate cancer. *Clin Cancer Res.* 2011;17:7645-7653.

8. Dietlein F, Kobe C, Neubauer S, et al. PSA-stratified performance of 18F- and 68Ga-labeled tracers in PSMA-PET imaging of patients with biochemical recurrence of prostate cancer. *J Nucl Med.* 2016.

9. Prasad V, Steffen IG, Diederichs G, Makowski MR, Wust P, Brenner W. Biodistribution of [(68)Ga]PSMA-HBED-CC in Patients with Prostate Cancer: Characterization of Uptake in Normal Organs and Tumour Lesions. *Mol Imaging Biol.* 2016;18:428-436.

10. Gunn RN, Gunn SR, Cunningham VJ. Positron emission tomography compartmental models. *J Cereb Blood Flow Metab.* 2001;21:635-652.

11. Ravert HT, Holt DP, Chen Y, et al. An improved synthesis of the radiolabeled prostate-specific membrane antigen inhibitor, [(18) F]DCFPyL. *J Labelled Comp Radiopharm.* 2016;59:439-450.

12. Windhorst AD, Linden TT, de Nooij A, et al. A complete, multipurpose, low cost, fully automated and GMP compliant radiosynthesis system. *J Labelled Comp Radiopharm* 2001;44:S1052-S1054.

13. Wondergem M, van der Zant FM, Knol RJJ, Lazarenko SV, Pruim J, de Jong IJ. (18)F-DCFPyL PET/CT in the Detection of Prostate Cancer at 60 and 120 Minutes: Detection Rate, Image Quality, Activity Kinetics, and Biodistribution. *J Nucl Med.* 2017;58:1797-1804.

14. Szabo Z, Mena E, Rowe SP, et al. Initial Evaluation of [(18)F]DCFPyL for Prostate-Specific Membrane Antigen (PSMA)-Targeted PET Imaging of Prostate Cancer. *Mol Imaging Biol.* 2015;17:565-574.

15. Boellaard R, van Lingen A, van Balen SC, Hoving BG, Lammertsma AA. Characteristics of a new fully programmable blood sampling device for monitoring blood radioactivity during PET. *Eur J Nucl Med.* 2001;28:81-89.

16. Frings V, Yaqub M, Hoyng LL, et al. Assessment of simplified methods to measure 18F-FLT uptake changes in EGFR-mutated non-small cell lung cancer patients undergoing EGFR tyrosine kinase inhibitor treatment. *J Nucl Med.* 2014;55:1417-1423.

17. Jansen BHE, Kramer GM, Cysouw MCF, et al. Healthy Tissue Uptake of (68)Ga-Prostate Specific Membrane Antigen (PSMA), (18)F-DCFPyL, (18)F-Fluoromethylcholine (FCH) and (18)F-Dihydrotestosterone (FDHT). *J Nucl Med.* 2019.

18. Schmidt K, Turkheimer F. Kinetic modeling in positron emission tomography. *The Quarterly Journal Of Nuclear Medicine And Molecular Imaging.* 2002;46:70.

19. Verwer EE, Oprea-Lager DE, van den Eertwegh AJ, et al. Quantification of 18F-fluorocholine kinetics in patients with prostate cancer. *J Nucl Med.* 2015;56:365-371.

20. Akaike H. A new look at the statistical model identification. *IEEE Transactions on Automatic Control.* 1974;19:716-723.

21. Schwarzenboeck SM, Rauscher I, Bluemel C, et al. PSMA Ligands for PET Imaging of Prostate Cancer. *J Nucl Med.* 2017;58:1545-1552.

FIGURE 1. A typical example of ^{18}F-DCFPyL uptake in a PCa metastasis (including the fit from the reversible two-tissue compartment model with a fixed k_4), blood, muscle and lung.

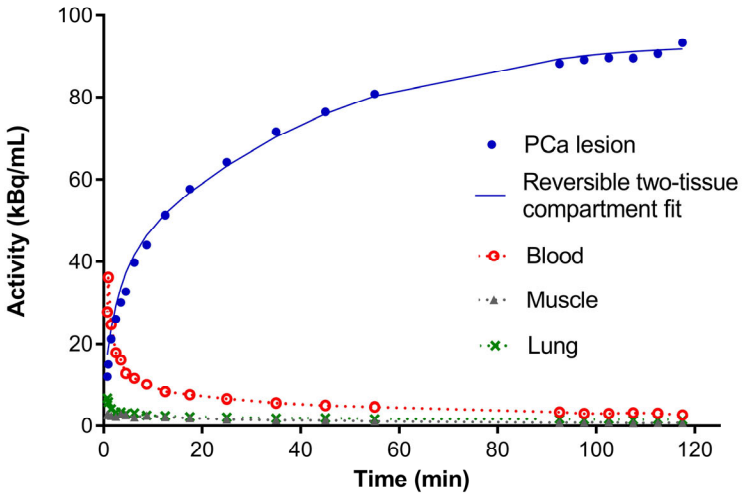

FIGURE 2. Fused images of PET and CT (radiotracer uptake in Bq/cc or SUV). Image-based Tumor-to-Blood ratio (TBR) are derived by normalizing tumor uptake (green Volume-of-Interest) with the activity in the ascending aorta (red Volume-of-Interest).

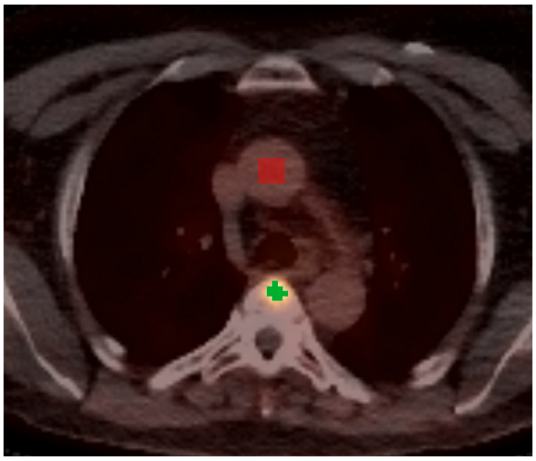

$$\text{Image-based TBR} = \frac{\text{Tumor Uptake}}{\text{Blood Pool Uptake}}$$

FIGURE 3. (A) Example of a typical Tumor-to-Blood ratio over time (B) Correlation of image-based Tumor-to-Blood ratios and K_i derived from pharmacokinetic modelling (reversible two-tissue compartment model).

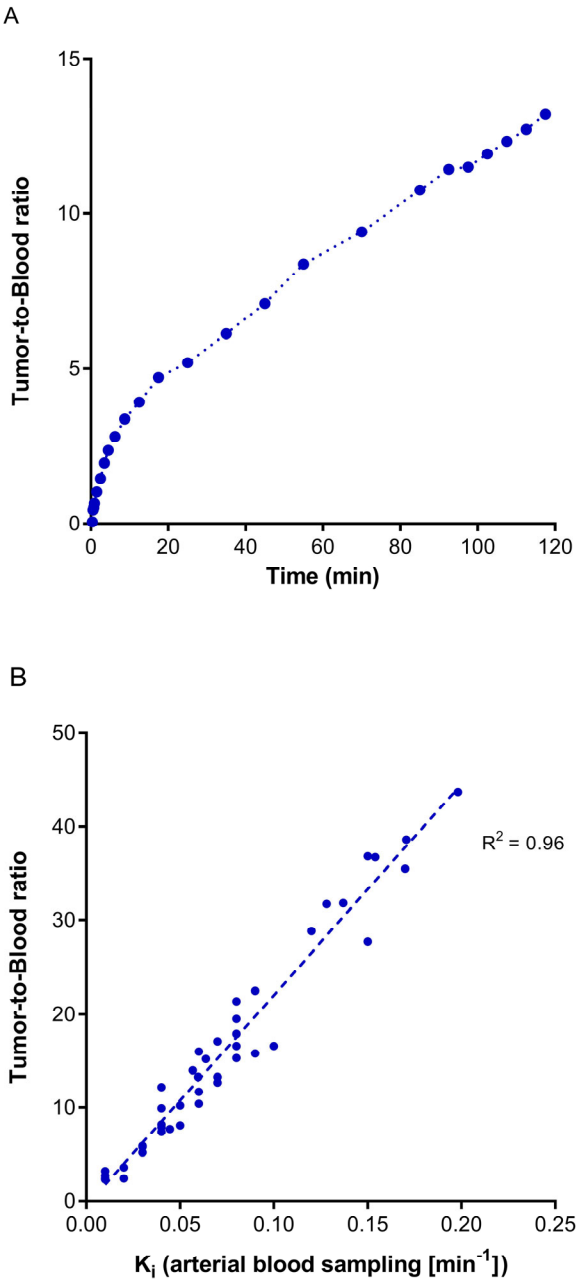

FIGURE 4. Varying individual relation of Standardized Uptake Values (normalized to body-weight) and K_i derived from pharmacokinetic modelling (reversible two-tissue compartment model).

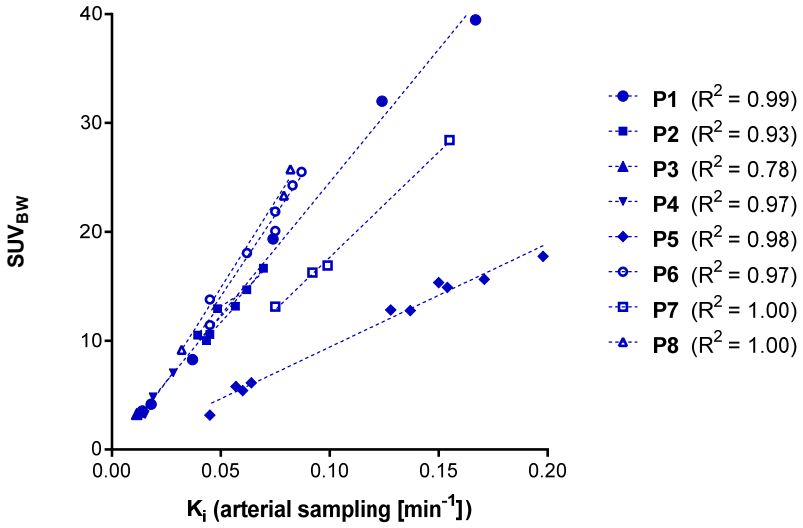

TABLE 1. Patient characteristics

Patient Characteristics	**Median**	**Range**
Age (years)	68	(56-81)
Initial Gleason score	9	(6-9)
PSA at time of scan (ng/ml)	473	(1.7-2792)
WHO performance score	0	(0-2)
Length (cm)	181	(171-191)
Weight (kg)	92	(64-119)
Prior treatment	*n*	%
Androgen deprivation therapy	7	88%
Docetaxel	7	88%
Enzalutamide / Abiraterone	5	63%

TABLE 2. Quantitative uptake metrics of ^{18}F-DCFPyL from full kinetic modeling and simplified methods. Medians and interquartile ranges.

parameter	median	IQR
K_1	0.14	0.08-0.26
k_2	0.09	0.07-0.11
k_3	0.07	0.06-0.08
k_4	0.02	*fixed*
V_b	0.08	0.07-0.14
K_i	0.06	0.04-0.09
V_T	4.58	3.76-5.13
Patlak K_i (30-120 min)	0.03	0.01-0.06
Logan V_T (30-120 min)	7.03	3.67-11.99
SUV_{BW}(30-60 min)	11.65	5.45-15.28
SUV_{BW} (90-120 min)	12.95	6.34-17.73
SUV_{BW} (110-120 min)	13.03	6.37-17.97
SUV_{AUC} (90-120 min)	0.06	0.04-0.11
Tumor-to-Blood (90-120 min)	13.83	7.29-23.05

TABLE 3. Correlation of K_i derived from pharmacokinetic modeling (two-tissue reversible model) with V_T and simplified methods.

Metrics	R^2	Slope	Intercept
V_T	0.96	182.2	-1.28
Patlak K_i	0.82	0.58	-0.00
Logan V_T	0.92	112.64	-0.69
SUV_{BW}	0.47	118.98	5.12
SUV_{LBM}	0.60	91.61	3.24
SUV_{AUC}	0.89	0.91	0.01
Tumor-to-Blood Ratio	0.97	222.06	-0.42
Image-based Tumor-to-Blood Ratio	0.96	226.08	-0.68

Supplemental Figure 1:
Plasma to Whole-Blood Ratios

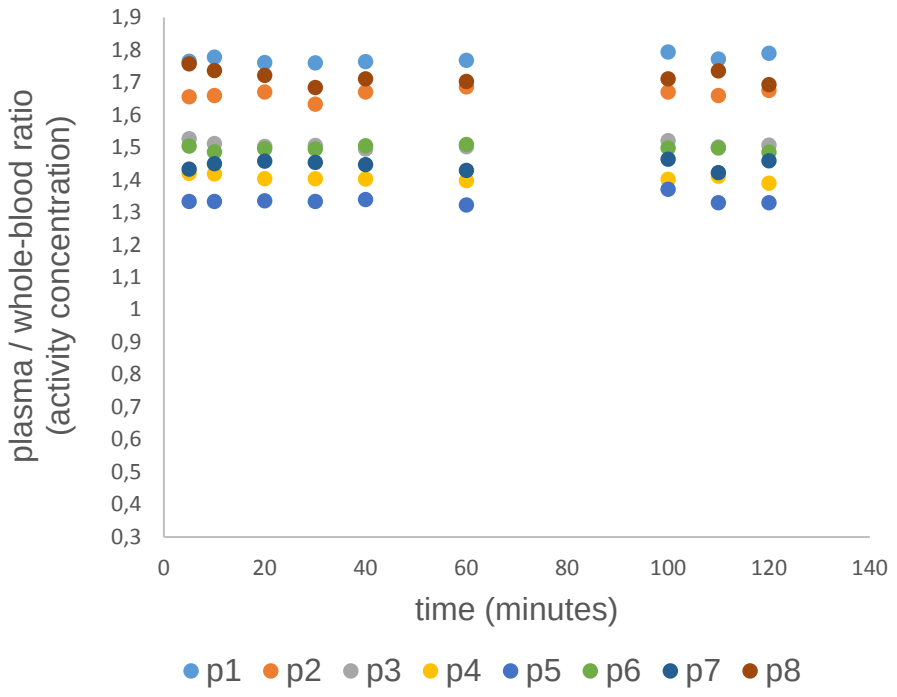

Supplemental Figure 2:
Correlation of Arterial and Venous Blood Activity

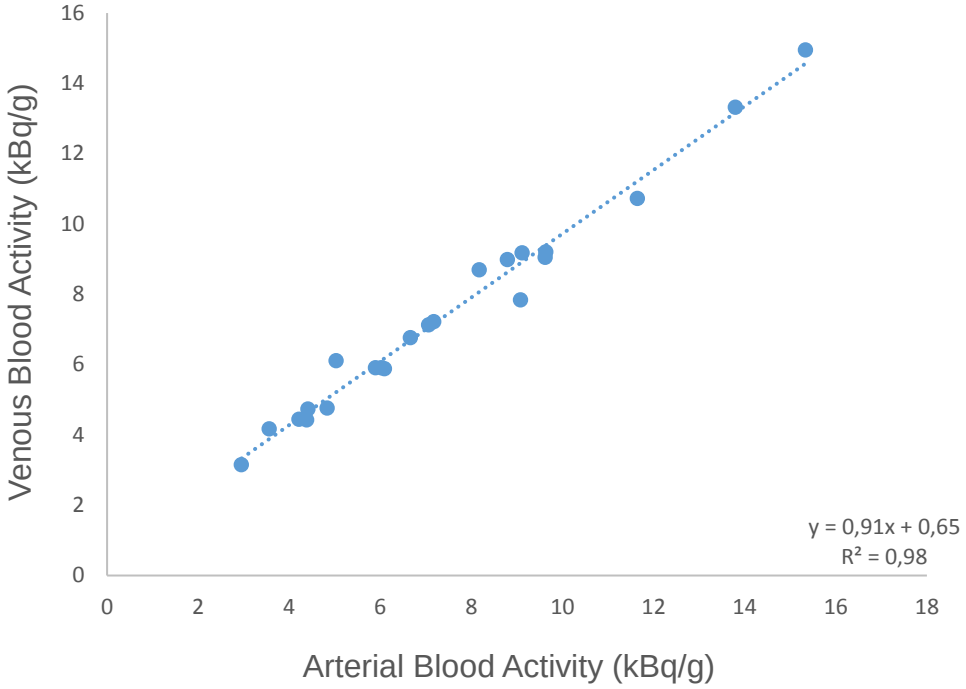

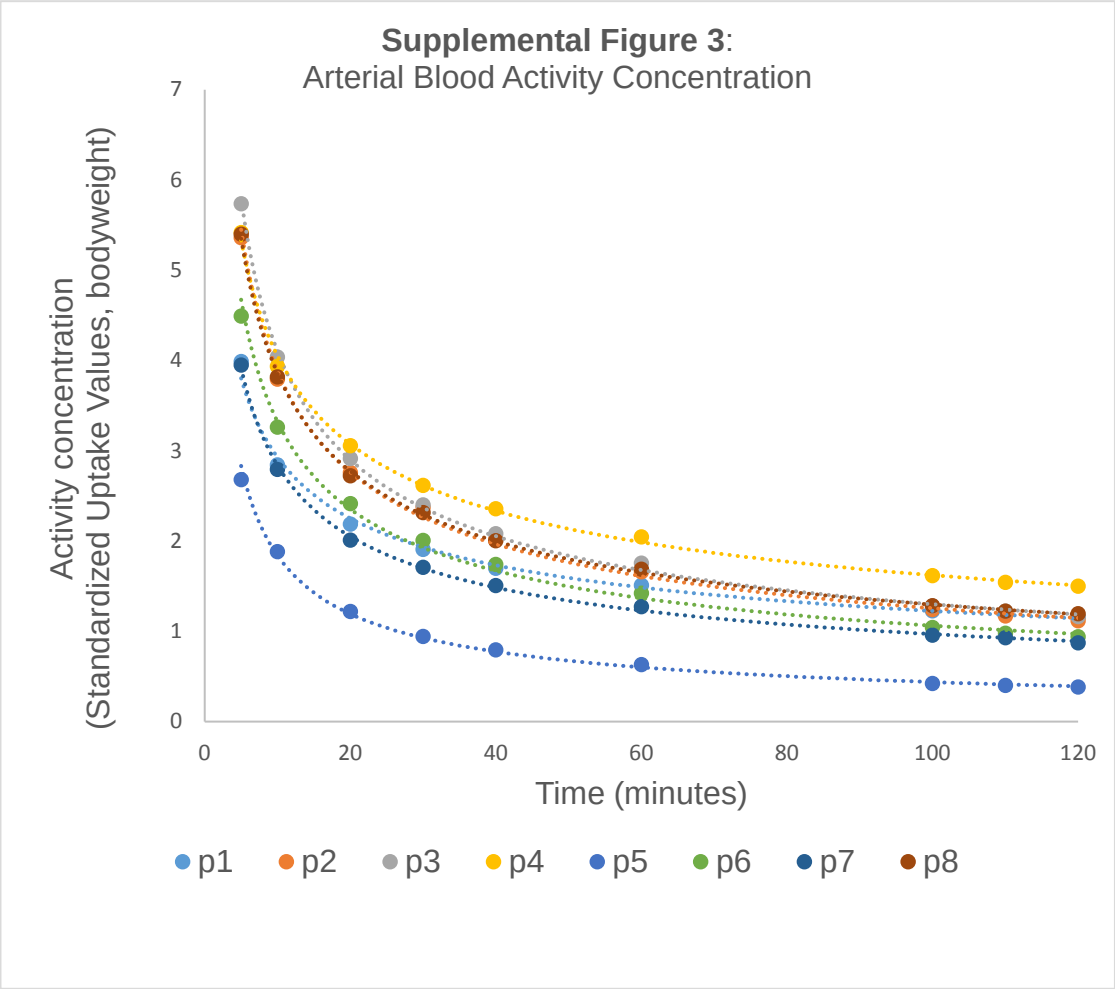
Supplemental Figure 3:
Arterial Blood Activity Concentration
Activity concentration
(Standardized Uptake Values, bodyweight)
0
1
2
3
4
5
6
7
0
20
40
60
80
100
120
Time (minutes)
p1
p2
p3
p4
p5
p6
p7
p8